Effects of an oscillating field on pattern formation in a ferromagnetic thin film: Analysis of patterns traveling at a low velocity

Kazue Kudo* and Katsuhiro Nakamura

Department of Applied Physics, Graduate School of Engineering, Osaka City University, Osaka 558-8585, Japan

Magnetic domain patterns under an oscillating field are studied theoretically by using a simple Ising-like model. We propose two ways to investigate the effects of the oscillating field. The first one leads to a model in which rapidly oscillating terms are averaged out and the model can explain the existence of the maximum amplitude of the field for the appearance of patterns. The second one leads to a model that includes the delay of the response to the field and the model suggests the existence of a traveling pattern which moves very slowly compared with the time scale of the driving field.

PACS number(s): 89.75.Kd, 75.70.Kw, 47.20.Lz, 75.10.Hk

I. INTRODUCTION

Rapidly driven systems have received considerable attention these days. Under a rapidly oscillating field, a state which is unstable in the absence of the oscillating field can be stabilized. One of the most simple and well-known examples is Kapitza's inverted pendulum and Landau and Lifshitz generalized the problem [1]. Their method has recently been applied to classical and quantum dynamics in periodically driven systems [2,3]. The method is also applied to stabilization of a matter-wave soliton in two-dimensional Bose-Einstein condensates without an external trap [4–6].

Magnetic domain patterns in a uniaxial ferromagnetic thin film, which usually show a labyrinth structure, exhibit various kinds of structures under an oscillating field. For example, the labyrinth structure changes into a parallel-stripe structure for a certain field [7,8]. In some other cases, several types of lattice structures can appear [9].

In this paper, we develop effective theories for slow motion of magnetic domain patterns under a rapidly oscillating field. Especially, we focus on traveling patterns as an example of slowly moving patterns. So far, there were few effective theories to describe such a slowly traveling pattern under a rapidly oscillating field. In experiments on a garnet thin film, we can observe a parallel-stripe pattern traveling very slowly compared with the time scale of the field in some cases [10]. A traveling mazelike pattern like Fig. 1 is also found in our numerical simulations.

Although traveling patterns appear in various kinds of systems, most works about them have been limited to the systems in the absence of an oscillating field [11–18]. The mechanism of such traveling patterns in one-dimensional (1D) systems was intensively studied in the 1980s as drift instabilities or parity-breaking instabilities [11–14]. In Ref. [11], secondary instabilities were discussed for several similar equations. By contrast, the authors of Refs. [12–14] gave no particular equation at first, but they considered symmetries of the system and assumed the form of the solution before deriving their equations. Almost 10 years after those papers, Price studied traveling patterns in 2D scalar nonlin-

ear neural fields where the nonlinearity is purely cubic and discussed constraints on the neural field structure and parameters to support traveling patterns [15]. He suggested that Swift-Hohenberg–type models will not support traveling patterns. However, moving patterns were actually observed in numerical simulations for a general complex Swift-Hohenberg equation in Ref. [16]. Our model has similar properties to those of the (real) Swift-Hohenberg equation. We will not use the method of Ref. [15] but that of Ref. [11] to explore the existence of a traveling pattern in a ferromagnetic thin film.

In fact, recently, domain walls under a rapidly oscillating field have been studied [19,20]. Michaelis *et al.* discussed the effects of rapid periodic oscillation of parameters in a Ginzburg-Landau (GL) equation by applying a multiscale technique and derived the averaged GL equation [19]; Kirakosyan *et al.* derived the averaged Landau-Lifshitz equation by employing the multi-time-scale expansion technique [20]. In those papers, they took into account higher harmonic oscillations. Although their methods cannot be directly applied to our model, our methods correspond to the lowest orders of their multi-time-scale expansions.

Our model is a simple 2D Ising-like model (see Refs. [21–24], and references therein), which has been used to simulate magnetic domain patterns. The numerical results simulated by the model show very similar properties to experimental ones [21–24]. We consider a scalar field $\phi(\mathbf{r})$, where $\mathbf{r} = (x, y)$. The positive and negative values of $\phi(\mathbf{r})$ correspond to the up and down spins, respectively. The Hamiltonian consists of four energy terms: Uniaxial-anisotropy energy H_{ani}, exchange interactions H_J, dipolar interactions H_{di}, and interactions with the external field H_{ex}. The anisotropy energy is given by
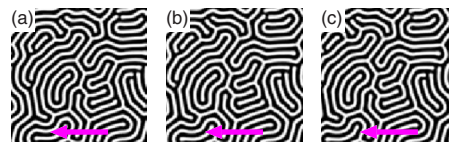

FIG. 1. (Color online) Snapshots of a traveling pattern under an oscillating field after (a) 5000 cycles, (b) 10000 cycles, and (c) 15000 cycles. The whole pattern is traveling to the left. The details are described in the Appendix.

*kudo@a-phys.eng.osaka-cu.ac.jp

036201-1

$$H_{\mathrm{ani}} = \alpha \int d\boldsymbol{r} \left(-\frac{\phi(\boldsymbol{r})^2}{2} + \frac{\phi(\boldsymbol{r})^4}{4} \right). \tag{1}$$

It implies that the anisotropy energy prefers the values $\phi(\boldsymbol{r}) = \pm 1$. The exchange and dipolar interactions are described by

$$H_J = \beta \int d\boldsymbol{r} \frac{|\nabla \phi(\boldsymbol{r})|^2}{2} \tag{2}$$

and

$$H_{\mathrm{di}} = \gamma \int d\boldsymbol{r} \, d\boldsymbol{r}' \, \phi(\boldsymbol{r}) \phi(\boldsymbol{r}') G(\boldsymbol{r}, \boldsymbol{r}'), \tag{3}$$

respectively. Here, $G(\boldsymbol{r}, \boldsymbol{r}') \sim |\boldsymbol{r} - \boldsymbol{r}'|^{-3}$ at long distances. The exchange interactions imply that $\phi(\boldsymbol{r})$ tends to have the same value as neighbors. On the other hand, the dipolar interactions imply that $\phi(\boldsymbol{r})$ tends to have the opposite sign to the values in a region at a long distance. Namely, H_J and H_{di} may be interpreted as short-range attractive and long-range repulsive interactions, respectively. Their competition leads to a domain structure with a characteristic length. The term from the interactions with the external field is given by

$$H_{\mathrm{ex}} = -h(t) \int d\boldsymbol{r} \, \phi(\boldsymbol{r}). \tag{4}$$

Here, we consider a spatially homogeneous and rapidly oscillating field:

$$h(t) = h_0 \sin \omega t. \tag{5}$$

From Eqs. (1)–(4), the dynamical equation of the model is described by

$$\frac{\partial \phi(\boldsymbol{r})}{\partial t} = -L_0 \frac{\delta(H_{\mathrm{ani}} + H_J + H_{\mathrm{di}} + H_{\mathrm{ex}})}{\delta \phi(\boldsymbol{r})} = L_0 \left\{ \alpha[\phi(\boldsymbol{r}) - \phi(\boldsymbol{r})^3] \right.$$
$$\left. + \beta \nabla^2 \phi(\boldsymbol{r}) - \gamma \int d\boldsymbol{r}' \phi(\boldsymbol{r}') G(\boldsymbol{r}, \boldsymbol{r}') + h(t) \right\}. \tag{6}$$

Hereafter, we fix $L_0 = 1$ and give the parameters α, β, γ, and h_0 as positive values.

In this paper, we propose two approximation methods to obtain the dynamical equation for slow motion. In both methods, we apply a part of Kapitza's idea that the dynamics under a rapidly oscillating field can be separated into a rapidly oscillating part and a slowly varying part [1]. In Sec. II, we derive the model whose rapidly oscillating part is averaged out on the basis of the Kapitza's idea about the time average of the fast motion. In Sec. III, we derive another model for the slow motion, considering the delay of the response to the field instead of taking a time average. After the derivation of the models, the instabilities of traveling patterns are investigated in both Secs. II and III. We discuss the details about the existence of a traveling pattern in Sec. IV. Conclusions are given in Sec. V.

II. TIME-AVERAGED MODEL

First of all, we assume that the variable $\phi(\boldsymbol{r})$ can be separated into two parts:

$$\phi(\boldsymbol{r}, t) = \Phi(\boldsymbol{r}, t) + \phi_0(t). \tag{7}$$

Here, $\Phi(\boldsymbol{r}, t)$ is a slowly varying term and $\phi_0(t)$ is a rapidly oscillating space-independent term. Substituting Eq. (7) into Eq. (6), we obtain

$$\frac{\partial \Phi(\boldsymbol{r})}{\partial t} + \dot{\phi}_0 = \alpha\{[\Phi(\boldsymbol{r}) + \phi_0] - [\Phi(\boldsymbol{r}) + \phi_0]^3\} + \beta \nabla^2 [\Phi(\boldsymbol{r})$$
$$+ \phi_0] - \gamma \int d\boldsymbol{r}' [\Phi(\boldsymbol{r}') + \phi_0] G(\boldsymbol{r}, \boldsymbol{r}') + h(t). \tag{8}$$

Let us consider only the rapidly oscillating space-independent part; then we have

$$\dot{\phi}_0 = \alpha(\phi_0 - \phi_0^3) - \gamma \phi_0 \int d\boldsymbol{r}' G(\boldsymbol{r}', 0) + h(t). \tag{9}$$

Here, we define $G(\boldsymbol{r}, 0) \equiv 1/|\boldsymbol{r}|^3$. Then, the integral in Eq. (9) is a constant, a_0:

$$a_0 = 2\pi \int_d^\infty \frac{dr}{r^2}. \tag{10}$$

Here, d is the cutoff length to prevent the divergence for $d \to 0$. It is also interpreted as the lower limit of the dipolar interactions. The solution of Eq. (9) should have the following form:

$$\phi_0 = \rho_0 \sin(\omega t + \delta), \tag{11}$$

where δ is a phase shift which comes from the delay of the response to the field. Substituting Eq. (11) into Eq. (9) and omitting high-order harmonics (i.e., $\sin 3\omega t$), we have

$$\omega \rho_0 \cos(\omega t + \delta) = \eta_0 \rho_0 \sin(\omega t + \delta) - \frac{3}{4} \alpha \rho_0^3 \sin(\omega t + \delta)$$
$$+ h_0 \sin \omega t, \tag{12}$$

where $\eta_0 = \alpha - \gamma a_0$. From Eq. (12), a pair of simultaneous equations is obtained:

$$-\omega \rho_0 \sin \delta = \left(\eta_0 - \frac{3}{4} \alpha \rho_0^2 \right) \rho_0 \cos \delta + h_0, \tag{13a}$$

$$\omega \rho_0 \cos \delta = \left(\eta_0 - \frac{3}{4} \alpha \rho_0^2 \right) \rho_0 \sin \delta. \tag{13b}$$

Eliminating δ from Eqs. (13a) and (13b), we obtain a cubic equation of $X \equiv \rho_0^2$:

$$\frac{9}{16} \alpha^2 X^3 - \frac{3}{2} \alpha \eta_0 X^2 + (\omega^2 + \eta_0^2) X = h_0^2. \tag{14}$$

Therefore, ρ_0 can be evaluated from Eq. (14) if the parameters α, η_0, ω, and h_0 are given.

Now, let us think about the slowly varying part. After substituting Eq. (11) into Eq. (8), we average out the rapid oscillation, closely following Kapitza's idea. Then, we obtain an equation for slowly varying domain patterns:

$$\frac{\partial \Phi(\mathbf{r})}{\partial t} = \alpha[\Phi(\mathbf{r}) - \Phi(\mathbf{r})^3] - \frac{3}{2}\alpha\rho_0^2\Phi(\mathbf{r}) + \beta\nabla^2\Phi(\mathbf{r})$$
$$- \gamma\int d\mathbf{r}'\Phi(\mathbf{r}')G(\mathbf{r},\mathbf{r}'). \tag{15}$$

The second term on the right-hand side of Eq. (15) is an extra term due to the time average. This term is essential to explore the effects of the rapidly oscillating field.

On the basis of Eq. (15), we will analyze the possibility of patterns traveling at a low velocity. Let us first choose the most simple moving stripe-type solution for Eq. (15):

$$\Phi(\mathbf{r},t) = A_0(t) + A_1(t)\sin[kx + b(t)]. \tag{16}$$

Substituting Eq. (16) into Eq. (15) and omitting high-order harmonics, we have

$$\dot{A}_0 + \dot{A}_1 \sin(kx + b) + \dot{b}A_1 \cos(kx + b) = \eta_0'A_0 + \eta_1'A_1 \sin(kx$$
$$+ b) - \alpha\left[A_0^3 + 3A_0^2A_1 \sin(kx + b) + \frac{3}{2}A_0A_1^2 + \frac{3}{4}A_1^3 \sin(kx\right.$$
$$\left. + b)\right]. \tag{17}$$

Here,

$$\eta_0' = \left(1 - \frac{3}{2}\rho_0^2\right)\alpha - \gamma a_0, \tag{18a}$$

$$\eta_1' = \left(1 - \frac{3}{2}\rho_0^2\right)\alpha - \beta k^2 - \gamma(a_0 - a_1 k), \tag{18b}$$

with a_0 given by Eq. (10), $a_1 = 2\pi$, and $k = |\mathbf{k}|$. Equation (17) leads to the following equations:

$$\dot{A}_0 = \eta_0'A_0 - \alpha\left(A_0^3 + \frac{3}{2}A_0A_1^2\right), \tag{19a}$$

$$\dot{A}_1 = \eta_1'A_1 - \alpha\left(3A_0^2A_1 + \frac{3}{4}A_1^3\right), \tag{19b}$$

$$\dot{b} = 0. \tag{19c}$$

Equation (19c) implies that the phase $b(t)$ in Eq. (16) shows no time dependence and that there is no traveling pattern with the simplest form like Eq. (16).

Next, let us consider a more generalized solution by incorporating the second harmonics:

$$\Phi(\mathbf{r},t) = A_0(t) + A_1(t)\sin[kx + b(t)] + A_{21}\cos\{2[kx + b(t)]\}$$
$$+ A_{22}\sin\{2[kx + b(t)]\}. \tag{20}$$

Substituting Eq. (20) into Eq. (15) leads to the following equations:

$$\dot{A}_0 = \eta_0'A_0 - \alpha\left(A_0^3 + \frac{3}{2}A_0A_1^2 + \frac{3}{2}A_0A_{21}^2 + \frac{3}{2}A_0A_{22}^2 - \frac{3}{4}A_1^2A_{21}\right), \tag{21a}$$

$$\dot{A}_1 = \eta_1'A_1 - \alpha\left(\frac{3}{4}A_1^3 + 3A_0^2A_1 + \frac{3}{2}A_1A_{21}^2 + \frac{3}{2}A_1A_{22}^2\right.$$
$$\left. - 3A_0A_1A_{21}\right), \tag{21b}$$

$$\dot{A}_{21} = \eta_2'A_{21} - \alpha\left(\frac{3}{4}A_{21}^3 - \frac{3}{2}A_0A_1^2 + 3A_0^2A_{21} + \frac{3}{2}A_1^2A_{21}\right.$$
$$\left. + \frac{3}{4}A_{21}A_{22}^2 - 6A_0A_{22}^2\right), \tag{21c}$$

$$\dot{A}_{22} = \eta_2'A_{22} - \alpha\left(\frac{3}{4}A_{22}^3 + 3A_0^2A_{22} + \frac{3}{4}A_{21}^2A_{22} + \frac{3}{2}A_1^2A_{22}\right.$$
$$\left. + 6A_0A_{21}A_{22}\right), \tag{21d}$$

and

$$\dot{b} = -3\alpha A_0A_{22}. \tag{22}$$

Here, η_0' and η_1' are given by Eq. (18a) and (18b), and

$$\eta_2' = \left(1 - \frac{3}{2}\rho_0^2\right)\alpha - 4\beta k^2 - \gamma(a_0 - 2a_1k). \tag{23}$$

This time, Eq. (22) implies that there can be a traveling pattern if $A_0 \neq 0$ and $A_{22} \neq 0$.

Now let us find a stationary point (SP) of Eq. (21a)–(21d) where $A_0 = 0$ or $A_{22} = 0$, and examine its linear stability. If the SP is unstable and both A_0 and A_{22} grow from zero, the pattern can start to travel. For the parameter values used to obtain Fig. 1, however, there are no SPs except for ones with $A_0 = A_{21} = A_{22} = 0$. We should note $A_1 = 0$ or $A_1^2 = 4\eta_1'/3\alpha$ at the SPs with $A_0 = A_{21} = A_{22} = 0$. Since A_1 must be real, $\eta_1' > 0$. Namely,

$$\rho_0^2 < \frac{2}{3\alpha}[\alpha - \beta k^2 - \gamma(a_0 - a_1k)]. \tag{24}$$

This condition gives an estimate of the maximum value of the field amplitude h_0 to observe a nonuniform pattern, as h_0 proves to be a monotonic function of ρ_0 for the parameter values in Fig. 1. In other words, if Eq. (24) is not satisfied, the only SP is $(A_0, A_1, A_{21}, A_{22}) = (0,0,0,0)$, which means that no pattern appears. At the SPs with $A_0 = A_{21} = A_{22} = 0$ and $A_1^2 = 4\eta_1'/3\alpha$, the Jacobian of Eq. (21a)–(21d) becomes

$$J = \begin{pmatrix} \eta_0' - 2\eta_1' & 0 & \eta_1' & 0 \\ 0 & -2\eta_1' & 0 & 0 \\ 2\eta_1' & 0 & \eta_2' - 2\eta_1' & 0 \\ 0 & 0 & 0 & \eta_2' - 2\eta_1' \end{pmatrix}. \tag{25}$$

The real parts of eigenvalues of Eq. (25) are $\Lambda_1 = -2\eta_1'$, $\Lambda_2 = \Lambda_3 = \frac{1}{2}(\eta_0' - 4\eta_1' + \eta_2')$, and $\Lambda_4 = \eta_2' - 2\eta_1'$. Note that Λ_1 is always negative. The others (Λ_2, Λ_3, Λ_4) also prove to be negative when $k \simeq 1$. In fact, the most preferable wave number of domain patterns is $k = 1$ for the parameter values in Fig. 1 (see Ref. [24] for details). Therefore, the present SPs

are stable and we cannot expect a traveling pattern in this case.

III. PHASE-SHIFTED MODEL

In this section, we consider another equation for slowly varying domain patterns instead of Eq. (15). We begin with Eqs. (7)–(12), (13a), (13b), and (14) again, but we will not take a time average. Instead, we take the delay of the response to the field into consideration. Substituting Eq. (11) into Eq. (8), we consider the equation as a discrete-time equation which is valid at $t=(2\pi/\omega)n$ with integers n. Then, we regard the discrete time as continuous. This procedure is justified when the field oscillation is rapid enough compared with the time scale of the slowly varying part. It is as if we take a sequence of snapshots at $t=(2\pi/\omega)n$ and take it as a movie. In fact, our numerical results in Fig. 1 are obtained by taking these kinds of snapshots. We thus obtain a new equation for slowly varying domain patterns:

$$\frac{\partial \Phi(\mathbf{r})}{\partial t} = \alpha(1 - 3\rho_0^2 \sin^2 \delta)\Phi(\mathbf{r}) + \beta\nabla^2\Phi(\mathbf{r})$$
$$- \gamma \int d\mathbf{r}' \Phi(\mathbf{r}')G(\mathbf{r},\mathbf{r}') - \alpha\Phi(\mathbf{r})^2[\Phi(\mathbf{r}) + 3\rho_0 \sin \delta]$$
$$+ C, \tag{26}$$

where

$$C = \eta_0\rho_0 \sin \delta - \alpha\rho_0^3 \sin^3 \delta - \omega\rho_0 \cos \delta, \tag{27}$$

with ρ_0 and δ evaluated from Eq. (13a) and (13b). Equation (26) has two extra terms due to the phase shift δ except for the constant C. One is linear and the other is nonlinear in Φ. The extra nonlinear term has an important role in the discussion of the existence of a traveling pattern.

Now, let us consider the stability of a traveling pattern on the basis of Eq. (26). When the simplest form, Eq. (16), is substituted into Eq. (26), we obtain the same result as Eq. (19c). Therefore, we proceed to choose the extended solution, Eq. (20). Substituting Eq. (20) into Eq. (26) leads to the following equations:

$$\dot{A}_0 = \tilde{\eta}_0 A_0 + C - \alpha\left[A_0^2(A_0 + 3\rho_0 \sin \delta) + \frac{3}{2}(A_0 + \rho_0 \sin \delta)(A_1^2 + A_{21}^2 + A_{22}^2) - \frac{3}{4}A_1^2 A_{21}\right], \tag{28a}$$

$$\dot{A}_1 = \tilde{\eta}_1 A_1 - \alpha\left[\frac{3}{4}A_1^3 + \frac{3}{2}A_1(A_{21}^2 + A_{22}^2) + 3A_0 A_1(A_0 + 2\rho_0 \sin \delta) - 3A_1 A_{21}(A_0 + \rho_0 \sin \delta)\right], \tag{28b}$$

$$\dot{A}_{21} = \tilde{\eta}_2 A_{21} - \alpha\left[\frac{3}{4}A_{21}^3 + \frac{3}{4}A_{21}(2A_1^2 + A_{22}^2) + 3A_0 A_{21}(A_0 + 2\rho_0 \sin \delta) - \frac{3}{2}(A_1^2 + 4A_{22}^2)(A_0 + \rho_0 \sin \delta)\right], \tag{28c}$$

$$\dot{A}_{22} = \tilde{\eta}_2 A_{22} - \alpha\left[\frac{3}{4}A_{22}^3 + \frac{3}{4}A_{22}(2A_1^2 + A_{21}^2) + 3A_0 A_{22}(A_0 + 2\rho_0 \sin \delta) + 6A_{21}A_{22}(A_0 + \rho_0 \sin \delta)\right], \tag{28d}$$

and

$$\dot{b} = -3\alpha(A_0 + \rho_0 \sin \delta)A_{22}. \tag{28e}$$

Here,

$$\tilde{\eta}_0 = (1 - 3\rho_0^2 \sin^2 \delta)\alpha - \gamma a_0, \tag{29a}$$

$$\tilde{\eta}_1 = (1 - 3\rho_0^2 \sin^2 \delta)\alpha - \beta k^2 - \gamma(a_0 - a_1 k), \tag{29b}$$

$$\tilde{\eta}_2 = (1 - 3\rho_0^2 \sin^2 \delta)\alpha - 4\beta k^2 - \gamma(a_0 - 2a_1 k). \tag{29c}$$

Equation (28e) suggests that there can be a traveling pattern if both $A_0 + \rho_0 \sin \delta \neq 0$ and $A_{22} \neq 0$ are satisfied.

Now let us think about the SPs of Eq. (28a)–(28e) where $A_0 + \rho_0 \sin \delta = 0$ or $A_{22} = 0$. For the cases with $k \simeq 1$ and the parameter set used in Fig. 1, we find that there are no SPs with $A_0 + \rho_0 \sin \delta = 0$. Therefore, we concentrate on SPs with $A_{22} = 0$, where Eqs. (28a)–(28e) lead to the following equations:

$$0 = \tilde{\eta}_0 A_0 + C - \alpha\left[A_0^2(A_0 + 3\rho_0 \sin \delta) + \frac{3}{2}(A_0 + \rho_0 \sin \delta)(A_1^2 + A_{21}^2) - \frac{3}{4}A_1^2 A_{21}\right], \tag{30a}$$

$$0 = \tilde{\eta}_1 A_1 - \alpha\left[\frac{3}{4}A_1^3 + \frac{3}{2}A_1 A_{21}^2 + 3A_0 A_1(A_0 + 2\rho_0 \sin \delta) - 3A_1 A_{21}(A_0 + \rho_0 \sin \delta)\right], \tag{30b}$$

$$0 = \tilde{\eta}_2 A_{21} - \alpha\left[\frac{3}{4}A_{21}^3 + \frac{3}{2}A_1^2 A_{21} + 3A_0 A_{21}(A_0 + 2\rho_0 \sin \delta) - \frac{3}{2}A_1^2(A_0 + \rho_0 \sin \delta)\right]. \tag{30c}$$

Here, we note that A_1 should not be zero. When $A_1 \neq 0$, Eq. (30b) leads to

$$A_1^2 = \frac{4\tilde{\eta}_1}{3\alpha} - 2[A_{21}^2 + 2A_0(A_0 + 2\rho_0 \sin \delta) - 2A_{21}(A_0 + \rho_0 \sin \delta)]. \tag{31}$$

Substituting Eq. (31) into Eqs. (30a) and (30c), we obtain a pair of nonlinear simultaneous equations for A_0 and A_{21}, which can be solved numerically.

At those SPs, the Jacobian of Eqs. (28a)–(28e) is

$$J = \begin{pmatrix} J_{11} & J_{12} & J_{13} & 0 \\ 2J_{12} & J_{22} & J_{23} & 0 \\ 2J_{13} & J_{23} & J_{33} & 0 \\ 0 & 0 & 0 & J_{44} \end{pmatrix}, \tag{32}$$

with the elements given by

$$J_{11} = \tilde{\eta}_0 - \alpha \left[3A_0^2 + 6A_0\rho_0 \sin \delta + \frac{3}{2}(A_1^2 + A_{21}^2) \right], \tag{33a}$$

$$J_{12} = -3\alpha A_1 \left(A_0 + \rho_0 \sin \delta - \frac{1}{2}A_{21} \right), \tag{33b}$$

$$J_{13} = -3\alpha \left[(A_0 + \rho_0 \sin \delta)A_{21} - \frac{1}{4}A_1^2 \right], \tag{33c}$$

$$J_{22} = \tilde{\eta}_1 - \alpha \left[\frac{9}{4}A_1^2 + \frac{3}{2}A_{21}^2 + 3A_0(A_0 + 2\rho_0 \sin \delta) - 3A_{21}(A_0 + \rho_0 \sin \delta) \right], \tag{33d}$$

$$J_{23} = 3\alpha A_1(A_0 + \rho_0 \sin \delta - A_{21}), \tag{33e}$$

$$J_{33} = \tilde{\eta}_2 - \alpha \left[\frac{9}{4}A_{21}^2 + \frac{3}{2}A_1^2 + 3A_0(A_0 + 2\rho_0 \sin \delta) \right], \tag{33f}$$

$$J_{44} = \tilde{\eta}_2 - \alpha \left[\frac{3}{4}(2A_1^2 + A_{21}^2) + 3A_0(A_0 + 2\rho_0 \sin \delta) + 6A_{21}(A_0 + \rho_0 \sin \delta) \right]. \tag{33g}$$

Equation (32) is a block-diagonal matrix. We can evaluate the real parts of the eigenvalues, Λ_1, Λ_2, Λ_3, for the upper-left 3×3 matrix as well as $\Lambda_4 = J_{44}$. The dependence of the real parts of the eigenvalues on the field amplitude h_0 is shown in Fig. 2. Here, we take the values of the parameters, α, β, and γ, used in Fig. 1. For $k=1.0$, all the real parts of the eigenvalues $(\Lambda_1, \ldots, \Lambda_4)$ are always negative. In other words, the SPs are stable and a traveling pattern cannot appear. For $k=0.83$, however, extra SPs appear in the region between $h_0 \simeq 0.35$ and $h_0 \simeq 1.5$. In that region, Λ_4 and one of the other three $(\Lambda_1, \Lambda_2, \Lambda_3)$ are positive. Incidentally, it is confirmed that $A_0 + \rho_0 \sin \delta \neq 0$ in the region. This result suggests that a traveling pattern can appear in a certain region of the field when $k=0.83$.

Using the above analysis, we show a stability diagram in Fig. 3. In the unstable area, where there is a branch with positive Λ_4, a traveling pattern can appear. In the stable area, where all the branches of Λ_4 have negative values, it cannot appear. The values of the parameters α, β, and γ are the same as ones in Fig. 1. The characteristic wave number k_0 depends on the ratio of β and γ (see Ref. [24] for details), and $k_0 = 1$ in our case. Though it is expected that $k \simeq k_0$, the actual characteristic length in the simulations is larger than
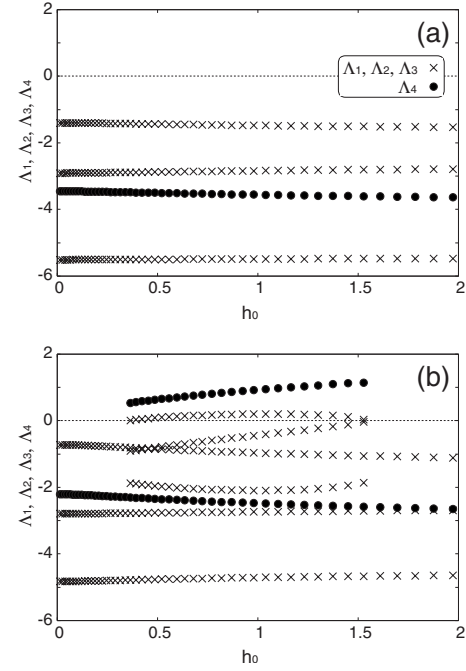

FIG. 2. The dependence of the real parts of the eigenvalues of Eq. (32) on the field amplitude h_0: (a) $k=1.0$ and (b) $k=0.83$.

$2\pi/k_0$. In other words, $k < k_0$ in the actual numerical results, although a domain pattern with a small k is not always realistic. Incidentally, the field larger than $h_0 \simeq 1.5$ may be meaningless since domain patterns should vanish under a strong field.

IV. DISCUSSION

The results in Fig. 2 suggest that a traveling pattern can exist for $k \leq 0.83$ but not for $k=1.0$. This can be interpreted as meaning that a traveling pattern should be a little fat. In fact, the actual wave numbers of domain patterns in our nu-
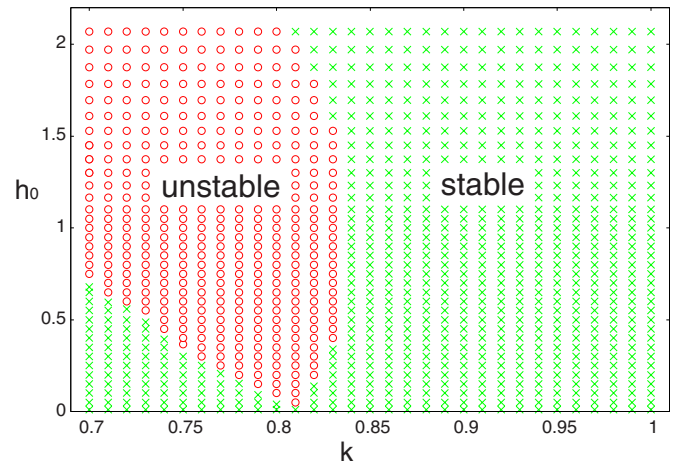

FIG. 3. (Color online) Stability diagram in k-h_0 space. In the unstable area (red-circle points), a traveling pattern can appear. In the stable area (green-cross points), the pattern cannot travel.

merical simulations are a little less than $k=1$, although $k=0.83$ seems too small. We can say that this fact partly supports the theoretical results given here.

We have used very simple approximations, i.e., perfect parallel-stripe structures without any distortion, to investigate the instabilities of a traveling pattern. That may be one of the reasons why the present analysis has suggested a traveling pattern with k smaller than that of the numerical results. In our simulations, the traveling patterns do not have a perfect parallel-stripe structure. If more complex and better approximations are employed, the actual traveling patterns exhibited by numerical simulations may be better explained.

In experiments, the perfect parallel-stripe structure is a realistic pattern. However, as mentioned above, the condition for a traveling pattern is tight even for such a simple structure. Traveling patterns with a more complex structure can be observed in experiments and the conditions of their appearance would be more complex than the present case. In any case, it is sure that a traveling pattern cannot appear without a rapid oscillating field.

V. CONCLUSIONS

We have proposed two ways to describe magnetic domain patterns moving slowly under a rapidly oscillating field. One gives a model in which rapidly oscillating terms are averaged out. The time-averaged model can explain the existence of the maximum values of the field where nonuniform domain patterns are preferable. The other gives a model which includes a phase shift as the delay of the response to the field. The phase-shifted model suggests the existence of a traveling pattern which moves very slowly compared with the time scale of the field. These two models have both merits and demerits. In other words, the approximations to be employed depend on the phenomenon under consideration. We should choose a method suitable for the analysis of the phenomenon to be investigated.

Although we have focused on a traveling pattern in this paper, these two methods are promising for applying to many other domain patterns under a rapidly oscillating field.

APPENDIX: NUMERICAL SIMULATIONS

The numerical procedures for time evolution are almost the same as those of Refs. [23,24]. For time evolution, we use a semi-implicit method: The exact solutions and the second order Runge-Kutta method are used for the linear and nonlinear terms, respectively. For a better spatial resolution, a pseudospectral method is applied. In other words, we numerically calculate the time evolutions of Eq. (6) in Fourier space:

$$\frac{\partial \phi_k}{\partial t} = \alpha[\phi - \phi^3]_k - (\beta k^2 + \gamma G_k)\phi_k + h(t)\delta_k, \quad \text{(A1)}$$

where $[\cdot]_k$ denotes the convolution sum and G_k is the Fourier transform of $G(r,0)$. Since we defined $G(r,0) \equiv 1/|r|^3$,

$$G_k = a_0 - a_1 k, \quad \text{(A2)}$$

where $k=|k|$ and

$$a_0 = 2\pi \int_d^\infty \frac{dr}{r^2}, \quad a_1 = 2\pi. \quad \text{(A3)}$$

In the simulations, we set $d=\pi/2$, which results in $a_0=4$.

In Fig. 1, the parameters are given as $\alpha=2.0$, $\beta=2.0$, and $\gamma=2\beta/a_1=2/\pi$. The frequency and amplitude of the field are $\omega=2\pi\times 5\times 10^{-2}$ and $h_0=0.8$, respectively. The simulations are performed on a 128×128 lattice with periodic boundary conditions. The snapshots in Fig. 1 are the domain patterns at (a) $5\times 10^3 T$, (b) $10\times 10^3 T$, and (c) $15\times 10^3 T$, where $T=2\pi/\omega$. If the amplitude is larger (for example, $h_0=0.9$, 0.95, etc.), we can see a traveling pattern with a different structure moves to a different direction.

[1] L. D. Landau and E. M. Lifshitz, *Mechanics* (Pergamon, Oxford, 1960).

[2] S. Rahav, I. Gilary, and S. Fishman, Phys. Rev. Lett. **91**, 110404 (2003); Phys. Rev. A **68**, 013820 (2003).

[3] S. Rahav, E. Geva, and S. Fishman, Phys. Rev. E **71**, 036210 (2005).

[4] H. Saito and M. Ueda, Phys. Rev. Lett. **90**, 040403 (2003).

[5] F. K. Abdullaev, J. G. Caputo, R. A. Kraenkel, and B. A. Malomed, Phys. Rev. A **67**, 013605 (2003).

[6] C. N. Liu, T. Morishita, and S. Watanabe, Phys. Rev. A **75**, 023604 (2007).

[7] S. Miura, M. Mino, and H. Yamazaki, J. Phys. Soc. Jpn. **70**, 2821 (2001).

[8] M. Mino, S. Miura, K. Dohi, and H. Yamazaki, J. Magn. Magn. Mater. **226–230**, 1530 (2001).

[9] N. Tsukamoto, H. Fujisaka, and K. Ouchi, Prog. Theor. Phys. **161**, 372 (2006).

[10] M. Mino (private communication).

[11] B. A. Malomed and M.I. Tribelsky, Physica D **14**, 67 (1984).

[12] P. Coullet, R. E. Goldstein, and G. H. Gunaratne, Phys. Rev. Lett. **63**, 1954 (1989).

[13] S. Douady, S. Fauve, and O. Thual, Europhys. Lett. **10**, 309 (1989); S. Fauve, S. Douady, and O. Thual, J. Phys. II **1**, 311 (1991).

[14] S. Fauve, S. Douady, and O. Thual, Phys. Rev. Lett. **65**, 385 (1990).

[15] C. B. Price, Phys. Rev. E **55**, 6698 (1997).

[16] J. Lega and N. H. Mendelson, Phys. Rev. E **59**, 6267 (1999).

[17] T. Okuzono and T. Ohta, Phys. Rev. E **67**, 056211 (2003).

[18] F. Sagués, D. G. Míguez, E. M. Nicola, A. P. Muñuzuri, J.

Casademunt, and L. Kramer, Physica D **199**, 235 (2004); D. G. Míguez, V. Pérez-Villar, and A. P. Muñuzuri, Phys. Rev. E **71**, 066217 (2005).

[19] D. Michaelis, F. Kh. Abdullaev, S. A. Darmanyan, and F. Lederer, Phys. Rev. E **71**, 056205 (2005).

[20] A. S. Kirakosyan, F. Kh. Abdullaev, and R. M. Galimzyanov, Phys. Rev. B **65**, 094411 (2002).

[21] E. A. Jagla, Phys. Rev. E **70**, 046204 (2004).

[22] E. A. Jagla, Phys. Rev. B **72**, 094406 (2005).

[23] K. Kudo, M. Mino, and K. Nakamura, J. Phys. Soc. Jpn. **76**, 013002 (2007).

[24] K. Kudo and K. Nakamura, Phys. Rev. B **76**, 054111 (2007).